Ballistics of Solid Rocket Motors with Spatial Burning Rate Variations

S. D. Heister*
Purdue University, West Lafayette, Indiana 47907

Introduction

THE solid rocket motor (SRM) ballistician has the job of predicting the chamber pressure and thrust history for both new and existing motors utilizing propellant burning rate and grain geometry, ambient conditions, and nozzle geometry. For motors which do have a test history, ballisticians introduce a constant "scale factor" to force predictions to match actual burn times of test units as well as a time varying multiplier to improve "pointwise" matching of the pressure history. This pointwise burning anomaly rate factor, or BARF, is usually established as a function of web distance since it is generally acknowledged that the factor accounts for spatial burning rate variations within the grain. This ubiquitous quantity has gone by several names through the years: hump factor, surface burn rate error (SBRE), and residual error to name a few.

Since the scale factor forces the average burning rate to match that in the test, the net integration of the BARF curve should have no effect on burning time. For most motors, the result takes on a hump-shaped appearance with maximum errors in burning rate usually being between 2–10%. Burning rate errors of this magnitude translate to errors in pressure of 3–15% due to the nonlinear dependence of pressure on this parameter.

Errors introduced due to the present technique for predicting ballistic response can require grain redesign and additional static tests. In addition, initial uncertainties in the ballistic prediction of maximum chamber pressure impacts the design of motorcase, nozzle, and insulation components since these parts must be designed for "worst case" predictions. Even if initial tests are deemed to be adequate, thrust history variations from the optimal design can cause losses in payload capability. Finally, spatial burning rate variations not normally considered by the ballistician can lead to changes in insulation exposure times when compared with current prediction methodologies.

This Note will investigate means to improve ballistic predictions by determining the contribution of spatially dependent burning rate variations to the BARF effect for a simple cylindrical-port motor. Background associated with research into BARF effects is provided in the next section, followed by a description of the technical approach. An analysis of a simple ballistic test motor follows this discussion, along with conclusions from the study.

While propellant strain, grain deformations during pressurization, local gas velocity effects, and possible migration of propellant constituents have all been theorized to contribute to BARF effects, the primary influence appears to be attributable to spatial variations in the local burning rate within the propellant grain. We make this assumption because the "hump shaped" character of the curve seems to be consistent across many motors of varying grain geometry, case deformations, and propellant formulations. In nearly all cases, spatial burning rate variations are attributed to one of two effects resulting from the rheological processes undertaken in loading the propellant into the motor. The two effects are 1) preferential orientation, or alignment of larger oxidizer particles as a result of shearing processes on the propellant as it flows to its resting place at some point within the grain; and 2) variations in local propellant composition—regions of high shear are assumed to be of higher binder content, thus causing observed variations in propellant burning rate.

While the early work of Bradfield[1] concentrated on variations in composition, Bradfield's limited success, combined with more recent evidence,[2] indicates that particle alignments are the most probable cause of spatial burning rate variations within the motor.

Numerous researchers[2,3] have documented the dependence of burning rate on oxidizer particle orientation. Particles aligned with their semimajor axis parallel to the direction of burning exhibit a higher burning rate than particles aligned perpendicular to the direction of burning. Propellant burning along an axis intermediate to these two extremes will exhibit an intermediate burning rate.

The fundamental cause for the increased rate for burning parallel to the "long" axis of the particles is due to increased conduction (to a greater depth) at the burn surface of propellant oriented in this fashion. Since the thermal conductivity of the oxidizer is greater than that of the binder, burning rates are governed by the oxidizer particles to a great extent. Stark and Taylor,[4] have demonstrated that the conductivity of the common oxidizer, ammonium perchlorate, is independent of direction within the crystal so with equal conduction rates, more heat will be transferred "in depth," thus amplifying the burning rate.

For a propellant flowing down the mandrel of a motor, shear forces will cause particles in the propellant to align parallel to wall surfaces. Radial flow between the mandrel and case wall will lead to alignments in the radial direction assuming that the shearing action generated during propellant flow causes large oxidizer particles to align with the direction of shear forces. Since the particles are much smaller than any characteristic flow distance, local alignment with the flow direction can be assumed for all but the smallest of rocket motors.

Similar arguments hold in the case where casting takes place at a single azimuthal location within the propellant annulus. In this case, the circumferential flow which results as the propellant fills a given annulus causes a shear stress which tends to align the particles semimajor axis perpendicular to the burn front at the inner and outer grain radii. Bradfield[1] analyzed BARF effects in small test motors filled in this manner by assuming Poiseuille flow around the annulus created by the mandrel and motorcase walls. Results of his study indicated that the point of maximum velocity associated with this flow correlated quite well with the location in the grain where the maximum BARF effect was observed.

Beckman and Geisler[5] noted a correlation (similar to Bradfield) of BARF effects with maximum flow velocity for ballistic test motors. These authors also noted that the effect was independent of aluminum level which indicates that oxidizer particles are the most probable cause for the behavior. Neilson and Miles,[6] noted that high pressures obtained during the early portion of several Space Shuttle solid rocket booster (SRB) firings were caused by changes in the size/shape characteristics of the ammonium perchlorate particles which might also be explained by a particle alignment scenario.

The influence of the casting apparatus has also been noted to cause measurable changes in the observed ballistic response. For example, Kallmeyer and Sayer[7] noted distinct changes in the SRB BARF curve when the forward and center segment casting apparatus was modified between development and qualification programs. These authors also noted a large degree of BARF repeatability among motors cast in a similar fashion. Lee et al.[8] attributed asymmetric erosion patterns in the Titan IV SRM to the two-pronged casting arrangement employed in the manufacture of this motor.

Presented as Paper 91-3394 at the AIAA/SAE/ASME 27th Joint Propulsion Conference, Sacramento, CA, June 24–26, 1991; received Jan. 10, 1992; revision received Aug. 6, 1992; accepted for publication Jan. 5, 1993.

*Assistant Professor, School of Aeronautics and Astronautics. Member AIAA.

Regardless of the mechanism, it has become apparent that ballistic predictions utilizing a spatial burning rate dependence have the potential of improving results from previous approaches. Recent measurements[2,9] on both subscale and full-scale motors has demonstrated a spatial burning rate dependence consistent with the arguments discussed above.

Technical Approach

Figure 1 highlights the geometry of a simple cylindrical-port SRM. All linear dimensions in Fig. 1 are presumed to be nondimensionalized by the motor diameter. This grain geometry can be prescribed in terms of the grain length L and the web fraction wf which represents the fraction of the motor radius loaded with propellant.

Since we are trying to determine the effects of a spatially dependent burning rate, we wish to construct an analytic function which prescribes variations in burning rate as a function of the variables w and X in Fig. 1. If our theory regarding the nature of these spatial variations is correct, we should expect that the radial burning rate would depend primarily on the web distance coordinate w. Variations in recession rate of this radial surface would depend on X only near the ends of the grain. Similarly, particle alignments as viewed from the axial surfaces could also be prescribed in terms of w alone if we are prepared to ignore "end effects."

Because the radial and axial surfaces are by definition 90-deg apart, we would expect that the response of the axial surface to be the inverse of that for the radial surface. In other words, when particles are aligned so as to give high radial burning rates, they must provide lower burning rates if viewed in the axial direction. This behavior has been confirmed experimentally in Ref. 9; results from this source have been reproduced as symbols appearing in Fig. 2 where web distances of zero and 100% correspond to the bore and case wall, respectively. Data in Fig. 2 have been nondimensionalized by the average burning rate across the web to insure that no scale factor effect is present.

In real applications, differences in casting and grain geometries between subscale test devices and full scale motors could also introduce a net scale factor. For example, if alignments

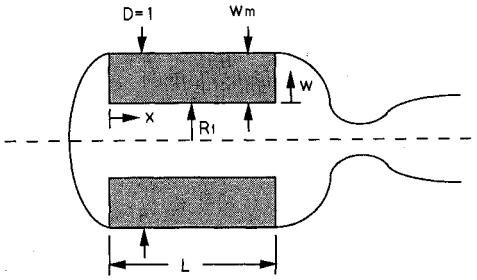

Fig. 1 Grain geometry for a simple cylindrical-port motor.

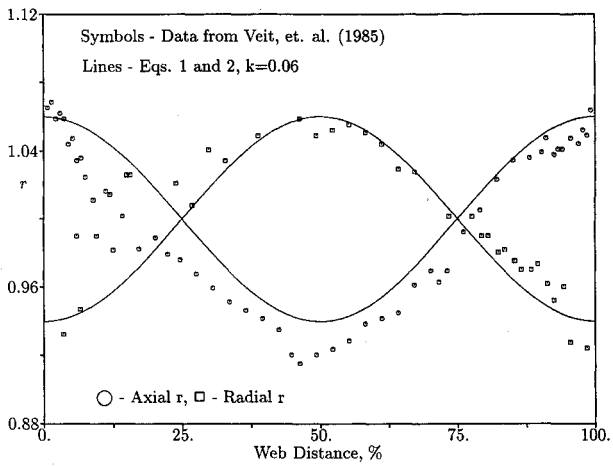

Fig. 2 Spatial burning rate variations.

were more prevalent in the full scale motor, we would expect a burning rate scale factor greater than unity. The full scale motor would burn faster (on average) than the subscale test device. This conclusion brings up an interesting point which in principle can explain why some motors exhibit rather large scale factors (in excess of 5%) when compared with subscale test results.

For the purposes of modeling the pressure dependence of the propellant burning rate, we shall assume that $r \propto p^n$, where n is the burning rate exponent. Assuming the spatial dependence can be introduced as a multiplicative factor, we may write

$$r = p^n[1 \pm kf(w)] \tag{1}$$

where k is an amplification factor and the function $f(w)$ describes the spatial variations present. Note that both the burning rate and pressure in Eq. (1) are presumed to be nondimensionalized by appropriate reference conditions.[10]

We require that the function $f(w)$ be a maximum at midweb and a minimum at either end of the web with no net integral (i.e., $\int_0^{w_m} f\,dw = 0$). A simple function with these properties is given by

$$f(w) = \sin\left[\pi\left(2\frac{w}{w_m} - \frac{1}{2}\right)\right] \tag{2}$$

Equation (1) is plotted using this $f(w)$ as the solid lines in Fig. 2 for $k = 0.06$. While the agreement between the model and the plotted data is not tremendous, the general spatial trends in burning rate are described by Eqs. (1) and (2). More elaborate fitting of the test data is not justified since we intend to apply the model to the simple grain design shown in Fig. 1. In practice, spatial variations could be employed by curve-fitting actual measurements or by correlating results from propellant casting fluid-dynamic models with some test data. Of course, the purpose of this analysis is to determine if such an approach might be fruitful.

A simple ballistics model[10] was generated presuming the spatial burning rate behavior indicated by Eqs. (1) and (2). Since we are attempting to discern differences of only a few percent, special care was taken to properly calculate massflow contributions from the curved axial surfaces resulting from this spatial burning rate law. Results of the model can then be compared with a "standard" ballistic calculation in which no spatial burning rate dependence is considered.

Discussion and Results

Results of calculations using the procedures discussed above are presented in Figs. 3–5. The influence of the spatially dependent burning rate on the dimensionless chamber pressure history is shown in Fig. 3 for a grain length of two and a web fraction of 0.6. The $k = 0$ curve in Fig. 3 would correspond to a result obtained by ignoring burning rate variations within the grain, while the burning rate model given by Eqs. (1) and (2) produces the other curves in Fig. 3. Note that the use of this burning rate model produces results similar to the use of a BARF curve, i.e., higher pressures during midburn with lower pressures near ignition and tailoff. Therefore, considering spatially varying burning rates has the potential for reducing the level of BARF effects and should improve chamber pressure predictions.

Figure 4 displays the grain burnback pattern for a web fraction and grain length of 0.8 and 1.6, respectively, for the case when $k = 0.1$. Note that even with this $\pm 10\%$ spatial burning rate variation, only slight curvatures are developed along axial surfaces. Since the burnbacks in Fig. 4 were plotted at equal time intervals, one can see the relatively larger radial burn rates in the midweb region. Also note that the high axial burn rates along the case wall leads to increased insulation exposure times when compared with a conventional analysis.

If we regard the $k = 0$ result in Fig. 3 as the prediction, and the other curves as measured values, the resulting BARF

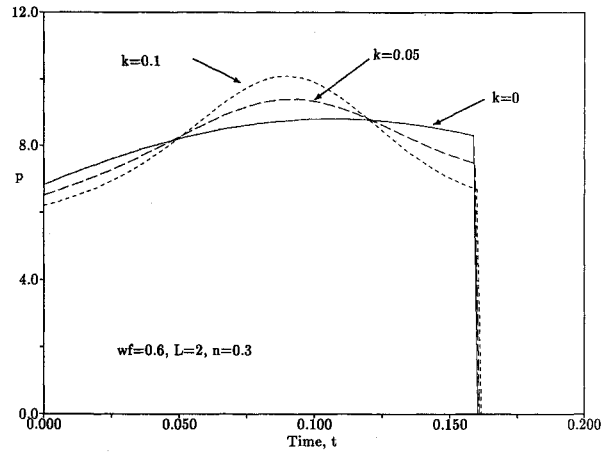

Fig. 3 Effect of spatial burning rate variations on chamber pressure.

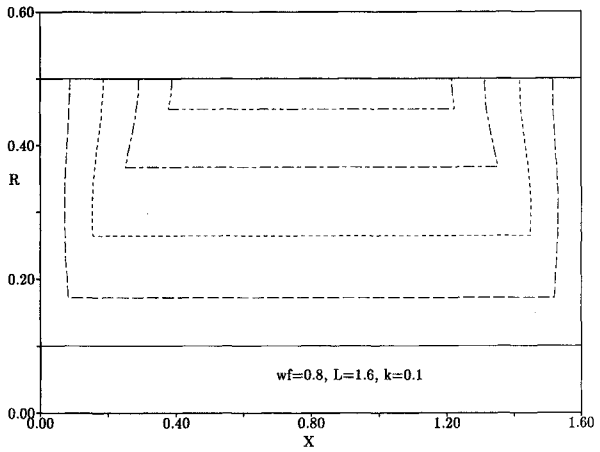

Fig. 4 Typical grain burnback pattern.

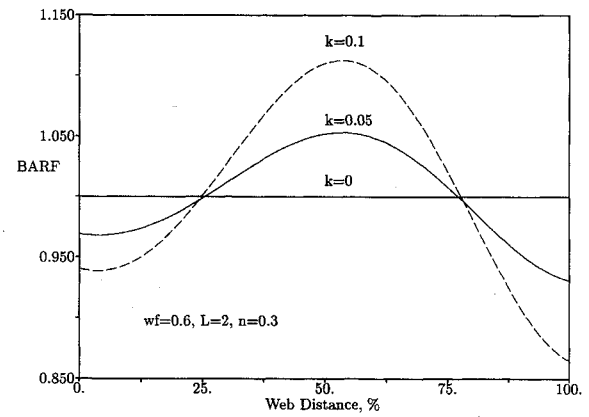

Fig. 5 Influence of spatial burning rate variation (factor k) on BARF curves.

curves can be generated by noting that BARF $\propto p^{(1-n)}$. Results of this calculation are shown in Fig. 5. This figure also indicates that moderate burning rate variations (e.g., only 1 or 2%) can lead to substantial BARF effects for a motor with a grain $L/D = 2$.

The model was also utilized to assess the effects of grain length and burning rate exponent on BARF predictions. Results indicate that end surface contributions become unimportant at a grain L/D greater than two such that all longer grains had similar BARF behavior.[10] In addition, increasing burning rate exponent had essentially no effect on the BARF curve for fixed grain geometry and k values since the BARF effect is the burning rate amplification required to match the observed pressure history.

Conclusions

Results for a simple cylindrical-port motor indicate that inclusion of spatial dependence of burning rate produces effects similar in nature (both qualitatively and quantitatively) to those normally attributed to the BARF. These results indicate that future ballistic predictions could be improved if such a spatially-varying burning rate model were incorporated within the predictions. Spatial variations along axial-facing propellant surfaces are of minor importance for grain $L/D > 2$, and burning rate exponent has no influence on the level of the BARF effect for fixed grain geometry and spatial burning rate variations.

References

[1]Bradfield, W. A., "Some Observations on the Effect of Viscosity During Casting on the Burning Rate Uniformity in the Web of the Cast Composite Propellant Charge," Australian Weapons Systems Research Lab., WSRL-0163-TM, Salisbury, Australia, June 1980.

[2]Miles, W. L., Christensen, W. N., and Gill, M., "Directional Burn Rate Bias in Large Diameter Motors," 1990 JANNAF Combustion Meeting, Cheyenne, WY, Oct. 1990.

[3]Koury, J. L., "Solid Strand Burn Rate Technique for Predicting Fullscale Motor Performance," Air Force Rocket Propulsion Lab.-TR-73-49, Oct. 1973.

[4]Stark, J. A., and Taylor, R. E., "Determination of Thermal Transport Properties in Ammonium Perchlorate," *Journal of Propulsion and Power*, Vol. 1, No. 5, 1985, pp. 409, 410.

[5]Beckman, C. W., and Geisler, R. L., "Ballistic Anomaly Trends in Subscale Solid Rocket Motors," 18th AIAA/ASME Joint Propulsion Conf., AIAA Paper 82-1092, Cleveland, OH, 1982.

[6]Neilson, A. R., and Miles, W. L., "Space Shuttle Solid Rocket Motor Reproducibility and the Apparent Influence of Propellant Processing Characteristics on Trace Shape," 25th Joint Propulsion Conf., AIAA Paper 89-2310, Monterey, CA, 1989.

[7]Kallmeyer, T. E., and Sayer, L. H., "Differences Between Actual and Predicted Pressure-Time Histories of Solid Rocket Motors," 18th AIAA/ASME Joint Propulsion Conf., AIAA Paper 82-1094, Cleveland, OH, 1982.

[8]Lee, H. S., Misterek, D. L., Davis, R. J., and Fukuda, M. K., "Asymmetric Sidewall Insulation Erosion for Titan 34D and Titan IV Solid Rocket Motors," 25th AIAA/ASME/SAE/ASEE Joint Propulsion Conf., AIAA Paper 89-2772, Monterey, CA, 1989.

[9]Veit, P. W., Landuk, L. G., and Svob, G. J., "Experimental Evaluation of As-Processed Propellant Grains," *Journal of Propulsion and Power*, Vol. 1, No. 6, 1985, pp. 494–497.

[10]Heister, S. D., "Influence of Propellant Rheology on Ballistic Response of Solid Rocket Motors," 27th AIAA/SAE/ASME Joint Propulsion Conf., AIAA Paper 91-3394, Sacramento, CA, 1991.

Modeling of Spray Droplets Deformation and Breakup

E. A. Ibrahim*
Tuskegee University, Tuskegee, Alabama 36088
and
H. Q. Yang† and A. J. Przekwas‡
CFD Research Corporation, Huntsville, Alabama 35805

Introduction

ONE of the most important processes that dominate spray combustion efficiency is spray drop deformation and

Received Sept. 8, 1992; revision received March 1, 1993; accepted for publication March 8, 1993.

*Assistant Professor, Mechanical Engineering Department. Member AIAA.
†Project Engineer. Member AIAA.
‡Vice President. Member AIAA.